PERGAMON

Journal of Atmospheric and Solar-Terrestrial Physics 63 (2001) 1117–1132

Journal of ATMOSPHERIC AND SOLAR-TERRESTRIAL PHYSICS

www.elsevier.nl/locate/jastp

The study of bulk plasma motions and associated electric fields in the plasmasphere by means of whistler-mode signals

D.L. Carpenter[a, *], A.J. Smith[b]

[a] *STAR Laboratory, EE Department, Packard Building, Stanford University, Stanford, California 94305-9515, USA*
[b] *British Antarctic Survey, Madingley Road, Cambridge CB3 0ET, UK*

Received 10 December 1999; accepted 6 June 2000

Abstract

Whistler-mode waves propagating to ground stations along geomagnetic-field-aligned paths provide powerful tools for investigating bulk motions of the magnetospheric plasma and thus the corresponding convection electric fields. Natural whistlers from lightning as well as signals from very low frequency (VLF) transmitters have been employed. The whistler method emphasizes measurement of temporal variations in the frequency versus time, or dispersion, properties of whistlers, while the transmitter method focuses upon measurement of the phase and group paths of fixed-frequency signal propagation. The methods depend upon wave properties that are sensitive to inhomogeneities in the geomagnetic field, and thus provide information on what are essentially cross-L plasma motions in a frame of reference rotating with the Earth. In addition, whistler data on the duskside plasmasphere bulge have been used to estimate values of the radial convection electric field (GSE Y direction) near dusk. In this topical review we discuss the development, beginning in the 1960s, of the whistler and transmitter methods, as well as a few of their geophysical applications. Whistlers have provided substantial new information on the spatially and temporally structured manner in which convection electric fields penetrate the plasmasphere, one example being the still unexplained reversal from inward to outward of the post-midnight radial flow direction following temporally isolated substorms. Whistlers have also been useful in identifying the plasmaspheric drifts associated with quiet-day electric fields of ionospheric dynamo origin and in showing that the E_y (duskward), component of the convection electric field in the outer plasmasphere is substantially larger near dusk than it is near mid-night. Whistler-mode signals from transmitters have been found to be a powerful means of tracking cross-L motions in the plasmasphere near $L = 2.5$ while separately identifying the effects of interchange fluxes with the ionosphere on the signal phase and group paths.

Keywords: Whistlers; Electric fields; Magnetospheric convection; Wave propagation; Signal processing; Remote sensing

1. Tracking plasma motions with whistlers

In this topical review we discuss the use of whistler-mode signals to measure bulk motions of plasma in the plasmasphere and the associated $-\mathbf{v}\times\mathbf{B}$ electric fields. Our emphasis is upon the history of the development of various methods and upon some examples of their application to geophysical problems.

The possibility of using whistlers launched by lightning to detect "cross-L" drift motions of the magnetospheric plasma, that is, motions in the direction of ∇B_m, where B_m is the minimum (essentially equatorial) value of the geomagnetic field, was first considered in the early 1960s. Strong evidence had been found that whistlers observed on the ground follow discrete magnetospheric paths between conjugate hemispheres (e.g. Smith, 1961a). Furthermore, theory had suggested that those paths take the form of geomagnetic-field-aligned enhancements in plasma density, acting much like light fibers in trapping wave energy and guiding it between conjugate hemispheres (Smith, 1961a). Whistler paths, thus observed

* Corresponding author. Fax: (650)-723-9251.
E-mail addresses: dlc@nova.stanford.edu (D.L. Carpenter), a.j.smith@bas.ac.uk (A.J. Smith).

1364-6826/01/$ - see front matter
PII: S1364-6826(00)00217-0

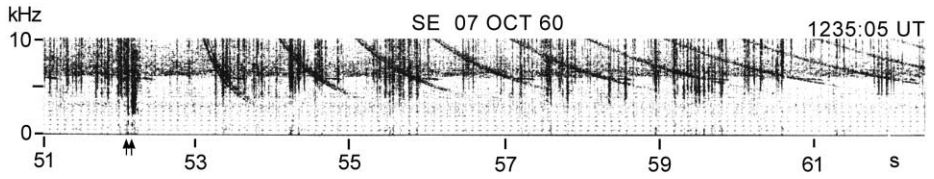

Fig. 1. Gray-scale record (0–10 kHz versus time) showing two closely spaced long enduring whistler echo trains recorded at Seattle, Washington on October 7, 1960 at 1235 UT (~0435 MLT). The radio impulses (sferics) associated with the originating lightning flashes are indicated by arrows below the record. The whistlers originated in the Northern Hemisphere and formed even-order echo trains. The successive echoes remained detectable after an estimated 200 hops along the magnetospheric path, or an interval of ~2 min (from Whistlers and Related Ionospheric Phenomena, R.A. Helliwell, Stanford Press, 1965).

in a reference frame rotating with the Earth, appeared to remain fixed in space for periods long with respect to the several-second duration of an individual whistler event, i.e. the f–t or dispersion properties of whistlers excited by successive lightning flashes could be identical within measurement accuracy. In this light and in view of work such as that of Axford and Hines (1961) on the phenomena of large-scale electric fields and associated magnetospheric convection, it seemed likely that whistler ducts were taking part in the large-scale bulk motions of the surrounding plasma and could thus provide a means of measuring the geoelectric fields associated with the motions. In the 1960s these fields were largely unexplored, and even today remain much more difficult to measure than are the major properties of the geomagnetic field.

One can imagine several approaches to the problem of tracking the motions of a whistler duct: (1) direction finding on the changing location of one of its endpoints in the ionosphere, (2) measurement of changes with time in whistler f–t properties that indicate the equatorial radius of the duct, (3) measurement of changes with time in the phase path of fixed-frequency whistler-mode signals propagating along the duct. Direction finding on path endpoints has been pursued with some success over the years (e.g. Leavitt et al., 1978; Machida and Tsuruda, 1984; Hayakawa et al., 1992) but has not yet been widely applied to the path drift problem. Most of the progress thus far has come from methods (2) and (3), and thus we emphasize those topics in this paper.

1.1. Initial whistler evidence of cross-L drifts

The first case investigated involved a series of whistlers recorded at 15-min synoptic intervals over a several hour period at Eights, Antarctica in 1963. Each whistler contained a single strong component that was followed by a series of echoes, much as in the case from Seattle, Washington illustrated in Fig. 1 on a record of frequency from 0 to 10 kHz versus time. In earlier work with such events it had been found that the two-hop travel time, the interval between successive echoes at a given frequency, remained unchanged from one echo to the next within a measurement accuracy of order 0.3% (Helliwell and Carpenter, 1961). Because of the echoing it was possible to measure the single-hop (hemisphere to hemisphere) travel time of the Eights whistler to an accuracy of better than 0.5% at a fixed frequency. Over the several-hour observation period, this travel time was found to decrease monotonically by ~10%. The decrease was tentatively interpreted as evidence of a reduction in path length as the field-aligned duct drifted inward through the geomagnetic field.

This interpretation was premature; changes in whistler travel time could be attributed to the interchange of ionization between the ionosphere and the overlying region as well as to changes in group path length associated with cross-L drift. In order to separately identify the role of cross-L drift, it was important to obtain a measure of the whistler path equatorial radius as a function of time. The frequency of minimum time delay of a whistler, or "nose frequency" f_n, had been shown by Smith (1961b) to be proportional to the minimum or equatorial gyrofrequency f_{Heq} along the whistler path, and thus could provide such a measure. That is, $f_n \approx k f_{Heq}$, where $k \approx 0.38$ for a diffusive equilibrium distribution of plasma along **B** in a dipole field (Angerami, 1966; Park, 1972). Fortunately, single-hop whistlers with clearly defined nose frequencies had been recorded in large numbers at Eights in 1963.

A key element in the work that followed was the ability to identify on spectrographic records the time of the causative lightning flash of a whistler, that is, the location of the particular impulsive signal or atmospheric that had propagated in the Earth-ionosphere waveguide from the source to the receiver. The causative atmospherics of one-hop whistlers received at Eights were often easily recognized on spectrograms, either through simple visual inspection or through comparison of spectra from several successive events (Carpenter, 1960). This was fortuitous, two contributing factors being a low-loss propagation path from the conjugate region, partially over sea water, and a lack of thunderstorm activity in the vicinity of the receiver.

An initial case was found involving multicomponent whistlers recorded at several-minute intervals over a ~3-h period beginning near local mid-night on July 7, 1963. As illustrated in the spectrograms of Fig. 2, each whistler exhibited a well-defined component with nose frequency near

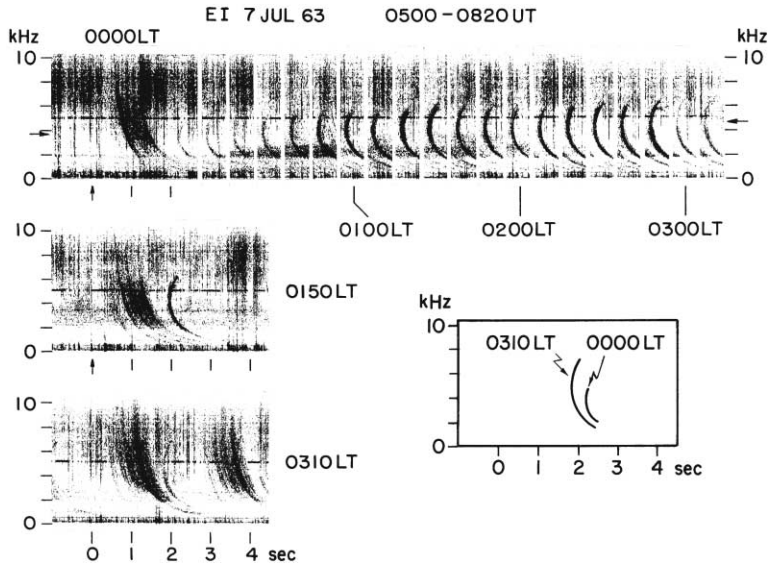

Fig. 2. Spectrograms showing changes with time in the f–t properties of a nose whistler component during a 3-h period following local mid-night. The recordings were made at Eights, Antarctica ($L \sim 3.9$) on July 7, 1963. At left from top to bottom are records of a multicomponent whistler at three times during the period. Across the top are spectrogram segments showing temporal variations in the component with nose frequency near 4 kHz (from Carpenter, 1966). See text for details.

$\sim$4 kHz. At the left from top to bottom are spectrograms of the entire multicomponent whistler at three times, 0000, 0150, and 0310 MLT. The three records are aligned vertically according to the time of the causative atmospheric (arrow or zero on the time scale). Extending to the right along the top panel are spectrogram segments of the component of interest, recorded at $\sim$10-min intervals over the $\sim$3-h period. Horizontal arrows at the left and right ends of the panel show the beginning and ending values of the nose frequency, while at the lower right is a tracing of the beginning and ending configurations of the component with respect to the time of the causative atmospheric. The overall increase in nose frequency implied an inward displacement of the equatorial crossing of the path by about $0.3R_E$, while the reduction in propagation time was consistent with expectations of an essentially electron-content-preserving motion of the flux tube. The decrease in path radius occurred near $L = 4$ in the outer plasmasphere and was consistent with what was being found about the nighttime inward displacements of the plasmapause (Carpenter, 1966).

The continuity of whistler activity along a drifting whistler duct was believed to be an example of magnetic-flux-preserving bulk motion of a geomagnetic-field-aligned plasma structure: if significant variations in electric potential had existed along the duct between conjugate topside ionospheres, the duct (considered as a plasma structure) could not have retained its field-aligned form and hence its properties as a wave guide, properties that Smith (1961a) and Helliwell (1963) had shown to be essential for downward ionospheric penetration.

1.2. Evidence of large-scale electric fields

The next step in development of the method involved simultaneous measurements on whistler paths spaced in equatorial radius. Cases of this kind could be used to demonstrate that the drifts being observed were part of a relatively large-scale convection pattern. Continuous records from Eights for 1965 were searched for multipath whistlers with clearly resolved nose frequencies and time separations of $\sim$1 min or less. In the 1963 Eights data, the fastest inward displacements of the plasmapause had been found to occur in the nightside during periods of moderate to severe substorm activity as indicated by the Kp index (Carpenter, 1966). In the light of the pioneering work by Akasofu (1964) on polar substorms, it was not surprising that the first clear example of fast inward multipath drifts appeared near local mid-night at the time of an individual substorm event. Fig. 3 shows the results as originally published by Carpenter and Stone (1967).

The upper panels of Fig. 3 display the H geomagnetic components recorded at the conjugate pair Byrd, Antarctica and Great Whale River, Canada ($L \sim 7$) and at Eights, Antarctica ($L \sim 3.9$). Magnetic bay activity at both Byrd and Great Whale, as well as increased absorption at Byrd, indicated the occurrence of a substorm. Below are plotted measurements of whistler path L value (equatorial radius in a dipole field) versus time, with each separately tracked whistler component denoted by a particular symbol. Fast inward drifts reaching speeds of $\sim$0.4–0.6 R_E h^{-1} began at $\sim$0620 UT ($\sim$0120 MLT), near the time of the bay

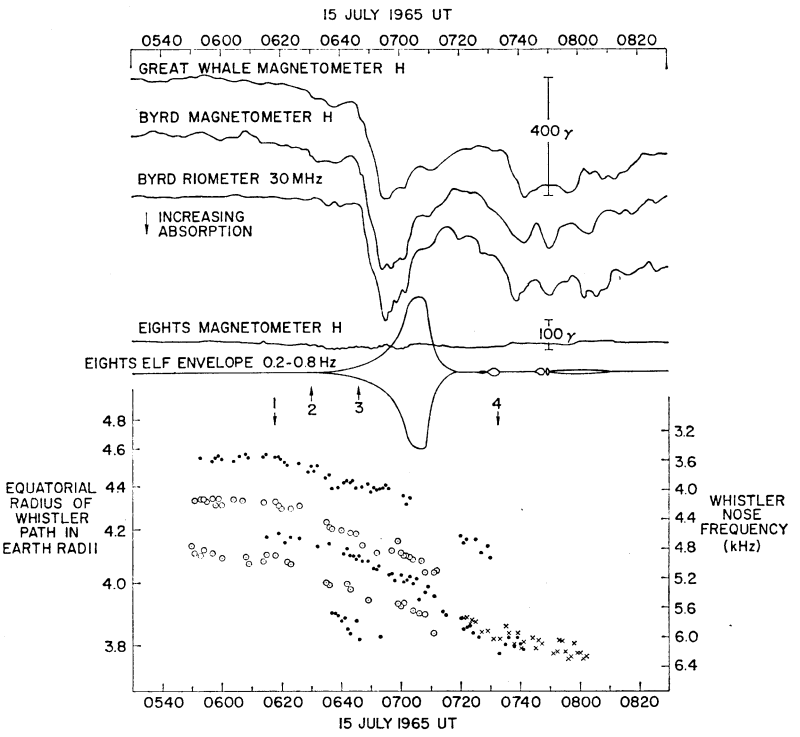

Fig. 3. Correlative records from a substorm period on July 15, 1965, showing substorm-associated decreases in the inferred equatorial radii of multiple whistler paths. Above the Eights, Antarctica whistler path data are records from the Byrd, Antarctica and Great Whale, Canada magnetometers, the Byrd riometer, and the Eights magnetometer and ULF detector (from Carpenter and Stone, 1967). See text for details.

activity at higher latitudes. The drifts occurred simultaneously on paths distributed over a range of $\sim 0.6 R_E$ in equatorial radius. Meanwhile, the Eights magnetometer showed little effect, although a Pc1 event occurred in apparent connection with the substorm.

1.3. Refinements and extensions of the method

The whistler method underwent a series of refinements and extensions in the late 1960s and throughout the 1970s. Fig. 4 shows some results of a more detailed analysis of the event of Fig. 3, in which the travel time to the whistler nose was scaled rather than the nose frequency itself (on a given whistler component, the nose travel time can in general be measured with greater accuracy than the nose frequency. This is suggested in Fig. 4 by the smallness of the short-term fluctuations in most of the individual time series).

Magnetic mid-night is marked by an M. The figure covers a 10-h period that includes the interval of Fig. 3 and displays the inverse of the measured nose travel time, t_n^{-1}. This quantity was chosen because its time rate of change $d(t_n^{-1})/dt$ was found to be approximately proportional to E_w, the westward component of the magnetospheric electric field (Carpenter et al., 1972). The constant of proportionality was only weakly dependent upon path L value, and the plot thus revealed a substantial degree of path-to-path similarity in the behavior of E_w.

The processing of data such as those displayed in Fig. 4 was labor intensive. Spectra of successive whistlers on 35 mm film were compared on a light box by means of tracing paper on which the form of a multicomponent whistler was traced for comparison with events nearby in time. These comparisons made it possible to identify the causative impulses of the whistlers and to mark the individual whistler components being tracked. The film was then projected onto a backlit screen equipped with an x–y digitizer, thus permitting the time of origin and dispersion information for each whistler to be scaled. The results were processed by means of a computer algorithm that smoothed and differentiated the data and then calculated the equatorial cross-L drift speed of each path and the corresponding values of E_w as functions of time. As applied to cases such as that of Fig. 4, the method was found capable of resolving fluctuations in E_w with period $T \sim 15$ min and rms amplitude as low as 0.05 mV m^{-1} (Carpenter et al., 1972).

The analysis method was later extended to lower L shells by a combination of curve fitting and travel time measurements at a fixed frequency (Carpenter et al., 1972). Fig. 5 shows examples of electric fields obtained in the case of Figs. 3 and 4 over L shells inside the plasmasphere ranging

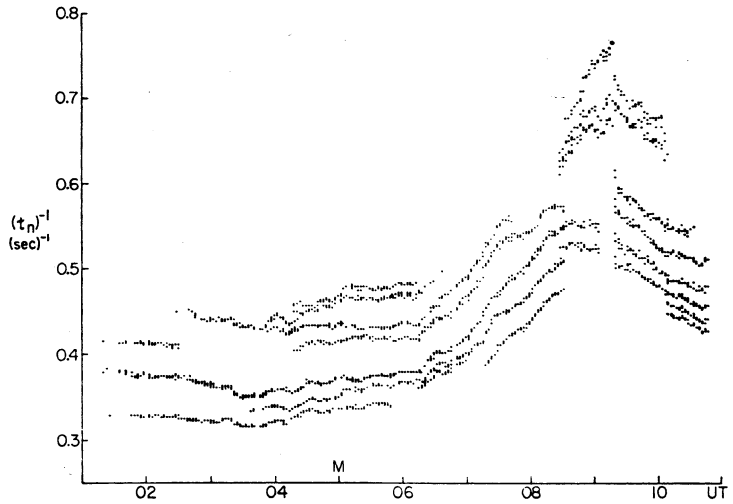

Fig. 4. Plot of variations in t_n^{-1} over an extended time period around the time of the substorm documented in Fig. 3, illustrating a high degree of spatial coherence of the path drift motions (except near 09 UT). On such a plot the slope of any data curve is approximately proportional to the westward electric field at the associated whistler path, the constant of proportionality being roughly the same for all paths. Magnetic mid-night is indicated by M (from Carpenter et al., 1972).

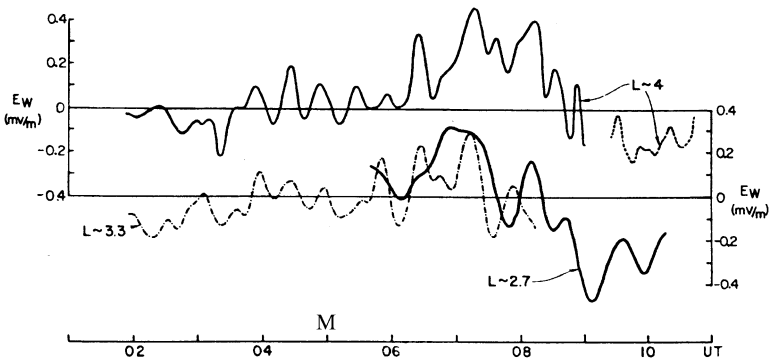

Fig. 5. Comparison of E_w variations observed in different L ranges during the convection event of Figs. 3 and 4. The data for $L\sim4$ were based upon direct measurements at the whistler nose, while those for $L\sim3.3$ and ~2.7 were based upon curve fitting and a time series of measurements at a fixed frequency (from Carpenter et al., 1972). Measurement uncertainty in data scaled from the whistler nose frequency (e.g. upper curves) was estimated to be $\pm25\%$ when $|E_w| > 2.0$ mV m^{-1} and $\pm.05$ mV m^{-1} when $|E_w| < 2.0$ mV m^{-1}. In the case of the fixed-frequency method (lower curves), these ranges should be roughly doubled (Carpenter et al., 1972).

from ~2.7 to ~4. The upper curves, for $L\sim4$, represent two of the components for which the nose frequency was directly observed, and the lower curves components for which the fixed-frequency method was used. Processing of the latter required additional smoothing owing to an increase with decreasing path L value in the size of associated scaling errors.

The whistler technique immediately yielded evidence of the complexity of substorm-associated electric fields. For example, it was found that fast sunward (nightside inward) drifts such as those illustrated in Fig. 3 were confined to local times near and following local mid-night (Carpenter et al., 1972). Furthermore, after temporally isolated substorms, the radial flow direction reversed from inward to outward (Carpenter et al., 1972; Carpenter and Akasofu, 1972; Carpenter and Seely, 1976). The outward drift could be roughly comparable in speed and duration to the preceding inward flow. This reversal effect is evident in Figs. 4 and 5 near 09 UT. Examples of reversals beginning at local times between $\sim$01 MLT ($\sim$06 UT) and $\sim$04 MLT ($\sim$09 UT), including the case of Figs. 4 and 5, are shown in Fig. 6. Local mid-night is again marked M on the UT scale. A particularly well-defined case occurred on July 4, 1963 (middle panel) and is repeated on the bottom panel of Fig. 7, where data from all the tracked components are

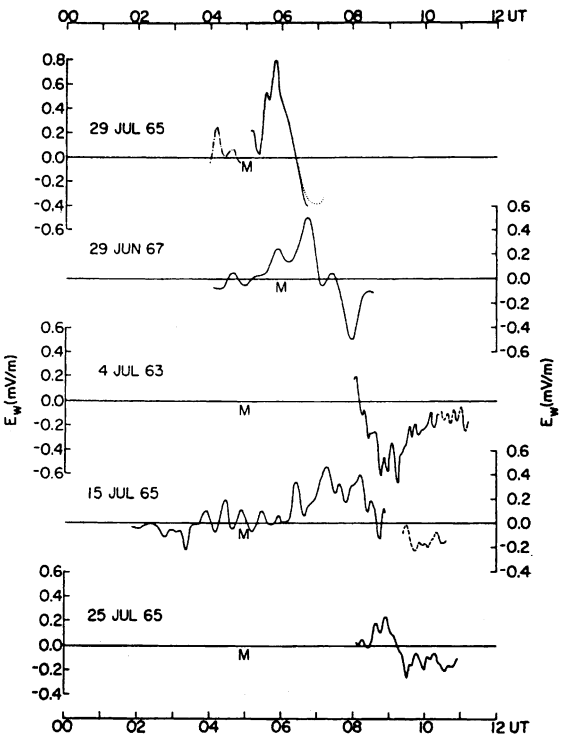

Fig. 6. Variations of E_w at the magnetospheric equator at $L\sim4$ during several periods of temporally isolated substorm activity. Magnetic midnight at the observing whistler station (Eights or Byrd, Antarctica) is marked by an M along the time scale. Each curve represents tracking of a particular whistler path by the nose frequency method (from Carpenter and Seely, 1976). See Fig. 5 caption for a note on measurement uncertainty.

shown (the continuous recording on this date was only available during the period 08–11 UT).

It was found that the most pronounced, order-of-1-h, inward drifts tended to develop at the time of the expansion phase of substorms, and not during a preceding "growth" phase. Although numbered arrows in Fig. 3 above the whistler path data appear to show a ~25-min delay between the onset of fast drifts (arrow 1) and the onset of the principal magnetic bay (arrow 3), later study (Carpenter et al., 1972) showed that while an initial ~20-min surge began at ~0618 UT (arrow 1), the principal, ~2-h-long, inward flow event actually began at ~0645 UT (arrow 3). This can be seen on the upper panel in Fig. 5.

Eights data from July 29, 1965, illustrated in Fig. 8, provided some particularly clear indications of temporal and spatial structure in cross-L plasma flow patterns. At the top are all-sky camera data from Byrd, Antarctica, as well as a ULF record from Eights, both indicating the onset of the expansion phase of a substorm at ~0522 UT. At the bottom are the H and D components from the Fredericksburg magnetometer, near the meridian of Eights. A westward deflection of the D component indicates the establishment of a strong field-aligned current system. In the middle is a plot of E_w from Eights whistlers (also shown on the top panel of Fig. 6). Fast inward flows were found to begin at ~0525 ± 5 min, which closely agrees with the Pi2 event (2d panel) and the time of auroral activation at higher latitudes. The reversal in flow direction, at ~0630 UT, occurred as the field-aligned-current activity decayed to low levels.

The reversal in flow direction has not been explained, although independent indications of the effect have been found in the properties of continuum radiation emissions observed on the Geotail satellite (Kasaba et al., 1988). The reversal

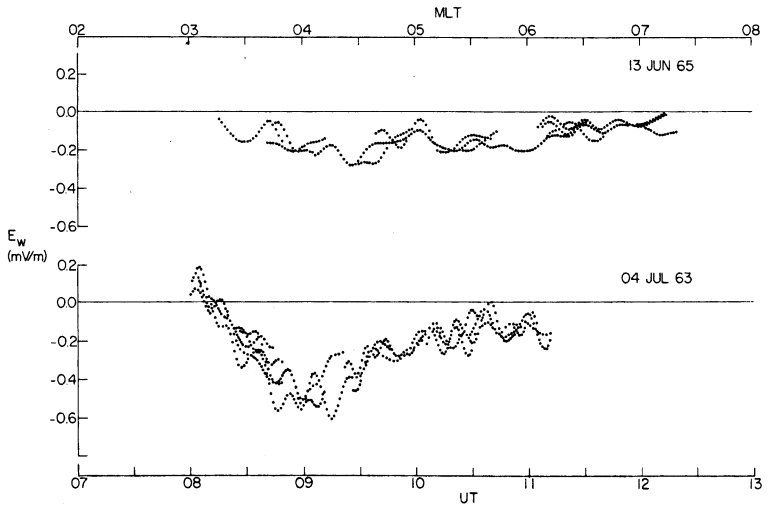

Fig. 7. Variations with time of E_w at $L\sim4$, illustrating differences in the predawn sector between an exceptionally quiet day (panel a) and the aftermath of a temporally isolated substorm (panel b). The data were obtained by differentiating the path position data of Fig. 9c and of Fig. 6, middle panel (from Carpenter and Seely, 1976).

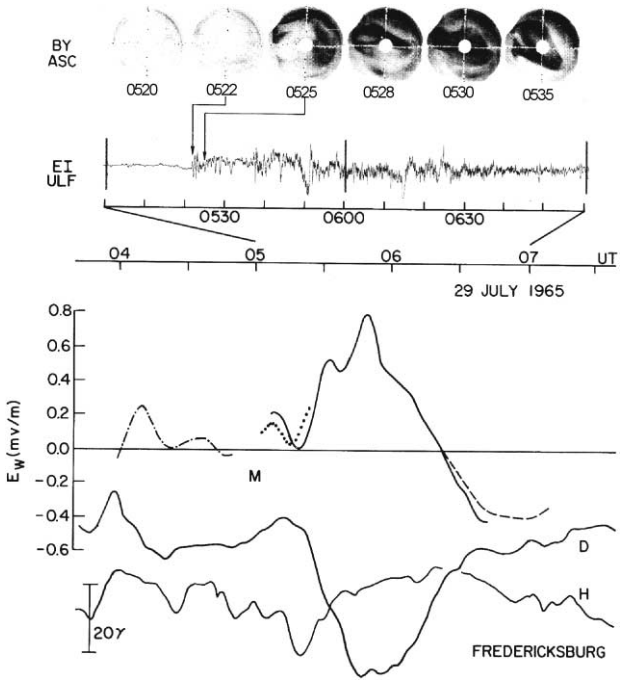

Fig. 8. Correlation plot of an isolated substorm on July 29, 1965, showing a steep rise in E_w in the outer plasmasphere at the time of the substorm expansion and a reversal in the sign of E_w as the substorm current system decayed. Above the Eights, Antarctica E_w data are Byrd, Antarctica all sky camera records and an Eights ULF record showing a Pi2 event. At the bottom are the D and H magnetometer components from Fredericksburg (from Carpenter and Akasofu, 1972).

may be related to the eastward electric field at subauroral latitudes in the dawn sector identified by Rostoker and Hron (1975) from magnetic perturbation data. It is also possible that some type of "overshielding" process is involved, in which the effects of field-aligned currents flowing at the inner edge of the plasma sheet or ring current produce a locally eastward electric field (outward drift) that persists after the currents associated with the inward drifts have decayed (e.g. Kelley, 1989).

1.4. Quiet day electric fields

Abundant whistler activity on geomagnetically quiet days near $L = 4$ in Antarctica made possible tracking of whistler ducts over extended time periods, as illustrated by two case studies in Fig. 9. (In plotting data on path radius, or L value, in a dipole field, it was at times convenient to use coordinates L^{-2} (or R^{-2}) versus time. On such plots (as in Figs. 9 and 10), the inferred east-west electric field is approximately proportional to the slope of any data curve, independent of the value of L (or R) (Carpenter et al., 1972).) The most clearly identified features in Fig. 9 are prenoon outward drifts and postnoon inward motions, which were interpreted as evidence of ionosphere dynamo effects (the SQ current system) (Carpenter and Seely, 1976; Carpenter, 1978). Details of E_w in the dawn sector for the case of Fig. 9b are shown in Fig. 7a for comparison to the shorter-duration, higher-amplitude flow reversal event of Fig. 7b.

An example of the interruption of quiet-day fields in the afternoon sector during a substorm is shown in Fig. 10, which displays whistler path radii versus time and the AE index. Until ~17 UT there was steady low-level substorm activity, and the cross-L flow direction was outward, as is normal for the prenoon sector under both moderately disturbed and quiet conditions (Carpenter et al., 1979). At ~17 UT (~12 MLT) the flow direction changed to inward as quieting began. During a substorm lasting from ~19 to 21 UT (~14–16 MLT) the flow reversed to outward, but then returned to the quiet-day inward direction as the AE index dropped to its pre-substorm level.

1.5. Effects of a nonstatic, nondipolar magnetic field

The analysis method as originally developed assumed that drifts occurred in a static dipole field. A study was later made of the effects on the method of departures from a dipole field and of changes in **B** with time as these might occur in connection with substorms (Block and Carpenter, 1974). In this work it was found that departures from a dipole field had relatively small effects on the analysis. When necessary they

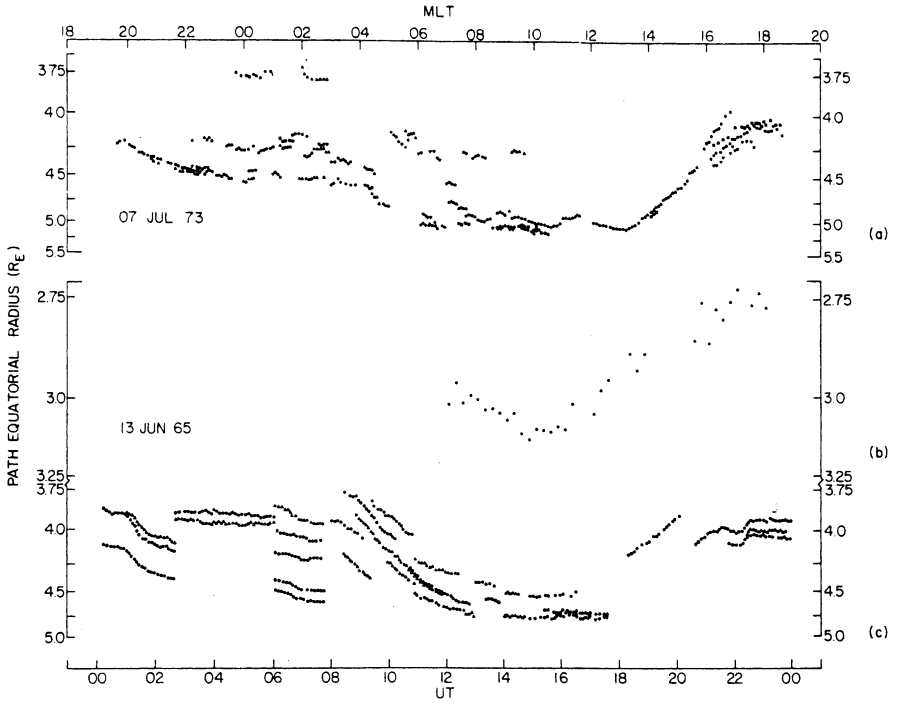

Fig. 9. Variations of whistler path equatorial radius with time during two exceptionally quiet 24-h periods: (a) July 7, 1973; (b) and (c) June 13, 1965 (from Carpenter and Seely, 1976). The data of (a) were recorded at Siple Station, Antarctica ($L \sim 4.4$), that of (b) at Eights.

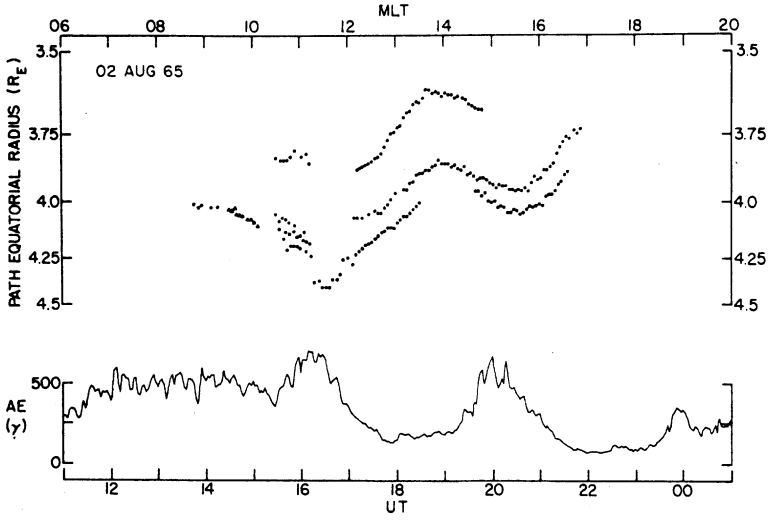

Fig. 10. Whistler path drifts in a dayside case illustrating a change in drift direction from inward to outward during a temporally isolated substorm (from Carpenter and Seely, 1976).

could be taken into account and would lead to corrections by factors of $< 30\%$ when a dipole field was assumed. Changes in **B** with time presented a more serious problem. Under such conditions the temporal change in equatorial gyrofrequency of a drifting whistler path would consist of two parts: a variation due to radial drifts of the path in the presence of the inhomogeneous **B** and a variation due to changes in **B** with time (recall that drifts in azimuth, or in outlying regions of nearly constant **B**, would not register as changes in f_n). If the changes in **B** with time could be known, their

contribution to the change in path gyrofrequency could be taken into account and the remainder of the change attributed to the total, potential plus induced, electric field. In a case study of a substorm in which the nightside **B** field appeared to increase rapidly on a time scale of ~15 min, the inferred total westward electric field was ~20% lower in amplitude than the field estimated on the assumption of a static dipole field. It was pointed out that the effects of fluctuating **B** could be more important on shorter time scales or during more severe disturbances than the one investigated ($K_p = 5-$).

Block and Carpenter (1974) noted that observed ~20-min fluctuations in E_w of ~0.1–0.2 mV m^{-1} during a quiet period prior to a substorm could have been associated with fluctuations in **B**. It was also pointed out that both equatorial and ionospheric measurements of electric fields are needed, since disturbances of the high altitude magnetosphere, such as by the ring current, are not readily observed in the electric field at ionospheric heights.

At the time of the study by Block and Carpenter (1974), applications of the whistler method during periods of fluctuating **B** were limited by lack of good observational information on **B** as well as models of its fluctuations. Now that greatly improved data and models are available, it would be appropriate to undertake new studies of the whistler technique as applied to periods of time-varying **B**.

1.6. Estimates of E_y in the dusk sector

Early interpretations of the global shape of the plasmasphere used the equatorial distance to a hypothetical stagnation point in the dusk sector as a measure of a large-scale dawn-to-dusk-directed electric field imposed on the interior of the magnetosphere by the solar wind (e.g. Vasyliunas, 1968; Kivelson, 1976). At the stagnation point, the imposed electric field was supposed to exactly cancel the corotation field associated with the Earth. In the whistler data there was no clear evidence of a stagnation point, at least as envisioned in theoretical models which combined a uniform dawn–dusk convection field with a corotation field. Instead, there were indications of decoupling of the main plasmasphere from the so-called bulge region of larger plasmasphere radius (Carpenter, 1966). That is, there was a fairly rapid spatial transition from a region dominated by rotation with the Earth to one strongly dominated by the convection electric field (Carpenter, 1970). As illustrated in the sketch of Fig. 11, this outer region exhibited an "abrupt" westward edge, extending from a distance R_A (afternoon plasmapause radius) to a distance of R_B (or beyond). The figure illustrates how the Eights station "equatorial viewing area" moved past the dusk meridian and "encountered" the "edge" of the bulge, in this case at time t_2. From data on the local time of such encounters during the 1963 and 1965 Austral winters, it was concluded that the outer region (beyond distance R_A) surged sunward during periods of increasing magnetic activity and moved backward, in the direction of the rotation of the Earth, as activity diminished. Using L ~4.5 as typical of the outer

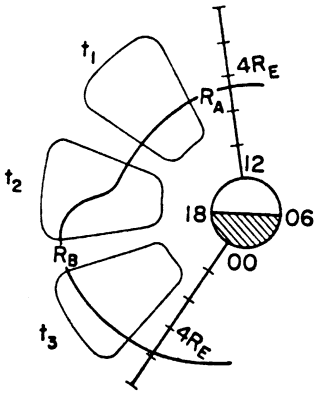

Fig. 11. Sketch of a dusk bulge encounter at dusk by a ground whistler station near $L=4$, showing the estimated equatorial "viewing area" of the station at three successive times. The plasmapause radius in the afternoon sector is marked R_A, while the larger radius during and immediately after the bulge encounter (usually less well defined in the data) is marked R_B (from Carpenter, 1970).

region, the electric field in the dawn–dusk direction (E_y) was estimated to be ~1–4 mV m^{-1} during substorms (as seen from the rotating Earth), about 4 times larger than the corresponding values observed in the post-mid-night sector by the whistler path drift method. A similar concentration of E_y fields near dusk has been found in double-probe electric field data from CRRES (e.g. Wygant et al., 1998).

1.7. Comparisons with other techniques

In 1978 a direct comparison was made between whistler data on cross-L plasma motions and incoherent scatter radar results on north-south plasma motions at ionospheric heights (Gonzales et al., 1980). The whistler data were acquired at Siple, Antarctica, conjugate to Roberval, Quebec, and represented an average of results for paths in the L range 3.5–4.7 near the longitude of the radar. The radar data were taken at Millstone Hill, Massachusetts and represented $L = 4.4$. Fig. 12 shows the northward and eastward components of ionospheric electric field determined by the radar (top and middle panels) and the eastward component of electric field at the equator inferred from the whistler drift data (bottom panel). The eastward electric field amplitude scales differ by a factor of 10 so as to approximately account for the magnetic-field mapping factor between the ionosphere and the equator (Mozer, 1970).

The eastward fields showed good agreement in the field direction over a 12-h period and, except near 0400 UT, suggested efficient mapping of the fields from the equator to the ionosphere. The good agreement during an isolated substorm near 0800 UT, in terms of mapping in a dipole-like field, suggested an essentially curl free condition of the electric field in the outer plasmasphere as well as essentially zero potential drop along the field lines of observation, at

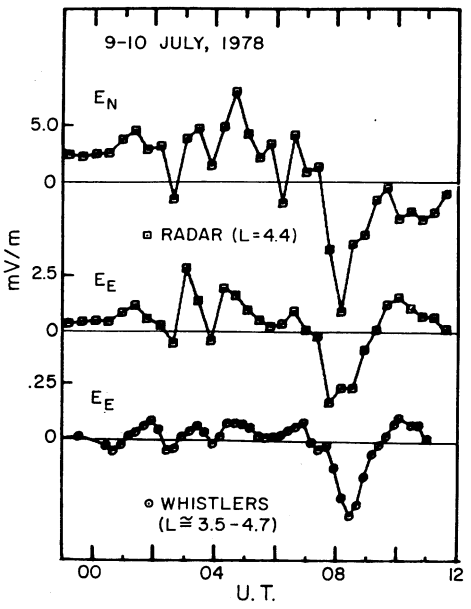

Fig. 12. Plasma drifts near the equator at $L\sim4.4$ obtained from whistlers are compared to corresponding data at ionospheric heights from the Millstone Hill radar, showing good agreement on the east-west electric field component before and during a small substorm. The top panel shows E_N, the north-south electric field from the radar, the middle panel the eastward field E_E from the radar, and the bottom panel E_E at the equator from whistlers (from Gonzales et al., 1980).

least on the time scale of 20 min over which the radar and whistler data were averaged.

Prior to the substorm near 0800 UT, double-probe electric field data were acquired on ISEE 1 in the near-equatorial region probed by the whistlers (Maynard et al., 1983). On a time scale of 20 min, the satellite results near $L = 4$ were in good agreement with the whistler and radar data.

2. Studies of plasma dynamics using fixed-frequency VLF whistler-mode signals

Since the early days of whistler research it was recognized that constant-frequency signals from VLF radio transmitters on the ground could travel along field-aligned magnetospheric paths much as do radio atmospherics from lightning (Helliwell and Gehrels, 1958). The observation of such whistler-mode signals in the region conjugate to the transmitter has been used as a complementary technique to that of lightning whistlers for deriving magnetospheric electric fields. The precisely known location, power and modulation format of VLF transmitters permits measurements not possible for whistlers, at the expense of the loss of frequency-dependent dispersion information.

2.1. Observations at $L\sim2.5$ of signals from communication transmitters

Early observations of whistler-mode signals from powerful VLF communications transmitters, such as NSS in Annapolis, Maryland, USA (Helliwell, 1965, Chapter 5), concentrated on occurrence data and the measurement of group delays and received power. Important results were obtained on transmission loss, especially in the ionosphere, and on the dependence of signal properties such as group delay on receiver location. McNeill (1967) developed a technique for measuring the Doppler shift of the 18.6 kHz whistler-mode signals from the NLK transmitter (at Seattle) received at Wellington, New Zealand. He found that whistler mode signals could be observed only when the ionospheric portion of the path was in darkness, otherwise D-region absorption suppressed the signal below the noise level. Even at night, the whistler-mode signals were typically 50 dB below the direct (subionospheric) signal. He showed that, like the group delay, the Doppler shift was a function of both the path drift and changes in path-integrated electron content, but that the former was the dominant contributor. Doppler shifts of both signs were observed, but positive shifts, corresponding to inward drifting paths, were more common. Shifts of up to 400 mHz were seen, of which ionospheric changes were estimated to contribute not more than 20 mHz. McNeill and Andrews (1975) analyzed 8 years of observations of NLK Doppler shifts at Wellington, and found a characteristic quiet-time behavior consisting of positive shifts at dusk which decreased during the night, consistent with $\mathbf{E}\times\mathbf{B}$ drifts under the influence of the S_q dynamo field. There were repeatable changes at dawn and dusk, believed to be due to interchange coupling fluxes between the plasmasphere and the ionosphere.

Thomson (1976a) was able to use occasional pulse transmissions from NLK to determine the Doppler shift and group delay simultaneously. An analysis of three candidate contributions to the Doppler shift showed that the effect of a changing magnetic field was too small to be measured, and that the effects of changing path length (due to cross-L drift) and changing flux tube electron content (due to ionosphere–magnetosphere coupling fluxes) could be separately estimated by comparing the ratio of Doppler shift Δf to rate of change of group time t_g. The ratio $dt_p/dt_g \equiv (dt_p/dt)/(dt_g/dt) = -(\Delta f/f)/(dt_g/dt)$ is about 1.7 for a stationary filling or depleting flux tube, but typically around 1 for a drifting tube with no coupling flux into or out of it. Applying this result to the data enabled Thomson (1976b) to measure quiet-time electric fields in the range $E_w \approx 0.0$–0.4 mV m^{-1} at $L=2.3$ (the L value was inferred from dispersion analysis of simultaneously observed whistlers). The method was subsequently applied (Andrews et al., 1978; Andrews, 1980), again using measurements on the NLK whistler-mode signal observed in New Zealand, to case studies in which cross-L drifts were seen to be typically positive after dusk, decreasing then increasing again

to a maximum near mid-night before decreasing to nearly zero at dawn. This behavior was consistent with inward $\mathbf{E} \times \mathbf{B}$ dynamo-driven drifts. Nighttime downward fluxes from the magnetosphere into the ionosphere were estimated to be of order 1×10^{-12} el m^{-2} s^{-1}.

Since it was difficult to distinguish different Doppler shifts for signals travelling along multiple paths with different L-shells and group delays, it was necessary to assume that one path was dominant and that the measured Doppler shift was the shift corresponding to that path. This shortcoming of the technique was overcome by Thomson (1981) with a new design of receiver. He used the fact that the direct subionospheric signal was highly coherent and much larger, typically by 50 dB, than the whistler mode and all sources of noise, and also that most of the powerful VLF transmitters such as NLK were by then transmitting in a precisely known and controlled MSK (minimum shift keying) modulation format. This enabled the transmitted signal to be demodulated, accurately reconstructed and then cross-correlated with the incoherent whistler mode signal plus noise (obtained by subtracting the direct signal from the total received signal). The result was digitally processed and averaged to suppress noise and obtain every 15 min the power and Doppler shift (in the range -500 mHz $< \Delta f <$ $+500$ mHz) separately for each of a set of different time delays in the range 0–1 s with a 5 ms resolution. In a further key development, a receiver of this type was deployed at Faraday, Antarctica (65°S, 64°W) (Smith et al., 1987) as well as in New Zealand at Dunedin (46°S, 171°E).

The advantages of the Faraday site were twofold. Firstly, although Faraday was situated at approximately the same geomagnetic latitude as Dunedin ($L\sim2.5$ versus $L\sim2.8$) it had a high geographic latitude. In fact it lay close to the meridian of the north geomagnetic pole, where the offset between geomagnetic and geographic latitudes is greatest. The constraint that at least one end of the path must be in darkness restricted the New Zealand observations to local nighttime only, whereas at Faraday in winter it was possible to operate throughout 24 h and thus measure plasmaspheric drifts and electric field at essentially all local times. Secondly, Faraday was in the only region on Earth conjugate to two relatively closely spaced powerful VLF communications transmitters operating at different frequencies: NAA (45°N, 68°W, 24.0 kHz) and NSS (39°N, 77°W, 21.4 kHz). This overcame an important disadvantage of single-frequency measurements compared with whistlers, for plasmaspheric diagnostics, namely that it was impossible to use dispersion analysis to infer the L value of the propagation path. In most cases similarities in Doppler shift and time dependence suggested that signals from both transmitters had traveled in the same duct, and it was then possible to calculate the propagation L-shell with some degree of confidence.

The principal remaining limitation to the technique, vis-á-vis the use of natural whistlers, was imposed by the half-gyrofrequency cut-off for ducted whistler-mode propagation. Typical high-powered VLF communications transmitters, with frequencies of 20 kHz or above, cannot propagate beyond $L\sim2.7$ and this restricts the field of view to the inner magnetosphere, in contrast to whistlers which can probe out to $L = 6$ and beyond (Carpenter, 1981). Until the advent of the global positioning system, there were transmissions between $\sim$10 and 13 kHz from the Omega navigational network, allowing the possibility of magnetospheric propagation out to $L\sim3.7$. However, the radiated powers of the transmitters were low, only $\sim$100 W in the case of the station in Forest Port, New York, and in those cases in which magnetospheric signals were reported, they showed evidence of nonlinear wave amplification (Kimura, 1968; Carpenter, 1968). As noted below, whistler-mode signals from the Siple experimental transmitter (Helliwell, 1974), which operated below 10 kHz, were often observed in the conjugate region in Canada, in most cases having propagated through the outer plasmasphere in the range $L = 3$–5 (Carpenter and Miller, 1976; Carpenter and Bao, 1983). The conditions necessary for Siple signal reception often involved nonlinear amplification processes which would make measurement of drift-related Doppler shifts difficult (Shklyar et al., 1992).

Fig. 13 shows an example of data from Faraday, from the first month of operation. Some typical features of the data are represented. In the intensity plots at the top, curved traces represent individual whistler ducts with group time delays changing with time. There were typically several ducts present, in this case with maximum and minimum group times delays differing by a factor of $\sim$2. Generally all the paths drifted in together in the same direction, which in this case reversed at about 8 UT. All the signals disappeared at dawn. The Doppler shifts are often positive when dt_g/dt is negative and vice versa (see particularly the feature centered near 8 UT and $t_g = 700$ ms), consistent with the time dependence being due to cross-L drifting of the propagation paths. The plots for the two transmitters are very similar, justifying the assumption that most paths were irradiated by both transmitters, and thus that the difference in t_g (which although small and not immediately apparent in the figure, can nevertheless be measured quite accurately, to within 1–2 ms) may be used to calculate dispersion and thence the L value of the path.

Saxton and Smith (1989) showed how to use the Faraday NAA and NSS data to determine separately the L value, cross-L drift velocity, and electron coupling flux for each of the observed whistler paths, in a way which was insensitive to the plasmaspheric and ionospheric electron density distribution models assumed. The distribution of L values was found to be peaked around $L = 2.5$, with 80% lying in the range 2.4–2.6. Thus Faraday could be considered as viewing a 0.2 L thick shell in the plasmasphere, centered on $L = 2.5$. The upper limit was determined by the gyrofrequency cutoff: $L = 2.63$ for NAA and 2.73 for NSS. Saxton and Smith (1989) studied nine quiet days in July 1986 to produce an average variation through 24 h. The

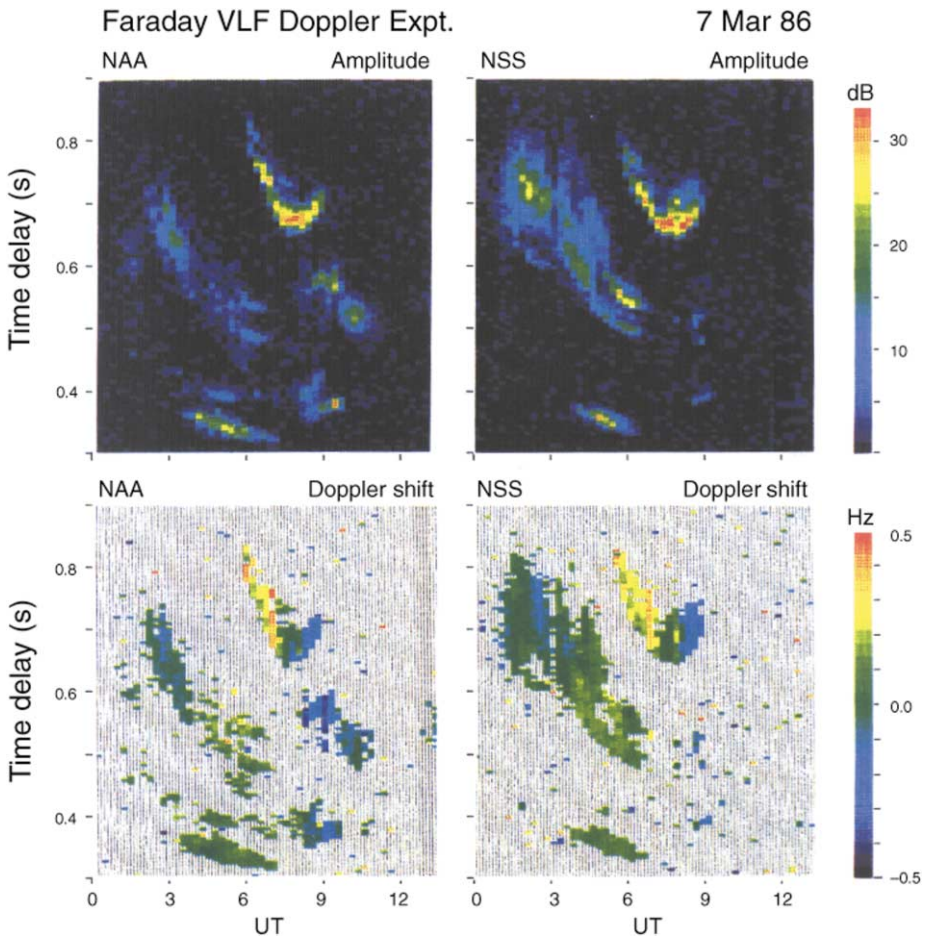

Fig. 13. Upper left panel: plot of NAA whistler mode intensity, shown qualitatively by the color scale, versus t_g and UT (LT = UT−4 h at Faraday). One pixel corresponds to 5 ms in t_g and 15 min in UT. Upper right panel: similar plot for NSS. Lower left panel: NAA Doppler shifts shown in colour for all signals exceeding a threshold; the t_g and UT scales are the same as for the upper panels. Lower right panel: similar plot for NSS. The factor of ∼2 differences in t_g values in this case suggests that the paths were at times distributed in L value over the range L∼2–2.7 (reproduced from Fig. 3 of Smith et al., 1987).

results are shown in Fig. 14 in terms of westward electric field E_w at $L = 2.5$. The field is eastward in the morning and early afternoon, and westward in the late afternoon until mid-night, then decreasing to near zero towards dawn. A similar study was carried out for moderately disturbed conditions using data from eight nights in June/July 1986 when K_p exceeded 2+ (Saxton and Smith, 1991). The results are shown in Fig. 15. Superimposed on this average behavior there were significant day-to-day variations. For example there were cases of enhanced drifts associated with discrete substorms; an example is shown in Fig. 5 of Saxton and Smith (1991).

The inferred electric fields were used as inputs to a self-consistent computer model of the ionosphere and plasmasphere (Balmforth et al., 1994b). This reproduced the experimental Doppler shift and group delay data and was also able to predict electric field-related changes which could not be observed directly. The model was later used in a study of the effects on the plasmasphere and ionosphere near $L = 2.5$ of two large magnetic storms, commencing 14 UT on May 2, 1986 and 22 UT on September 11, 1986 (Balmforth et al., 1994a). Faraday data from NAA and NSS were used to estimate the $\mathbf{E} \times \mathbf{B}$ drifts for input to the model. Fig. 16 shows the inferred azimuthal electric field for the September event, which after a small eastward excursion immediately after the sudden storm commencement became strongly westward (inward drift). It was not possible to get continuous electric field estimates throughout the storm because of the absence at times of well-defined whistler-mode signals (possibly due to the disruption of sufficiently

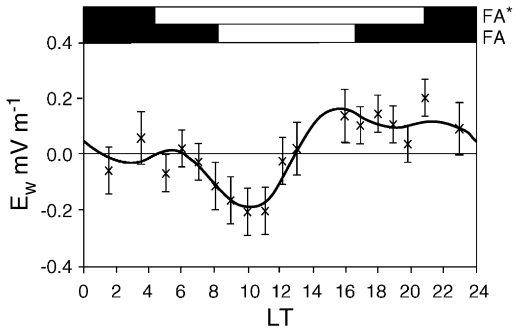

Fig. 14. The variation with local time of the average eastward electric field at $L = 2.5$ for nine quiet days in July 1986, obtained from NAA and NSS whistler-mode observations made at Faraday, Antarctica. The solid curve is a third-order harmonic fit to the data. The white sections of the bars along the top of the plot indicate, for Faraday and its conjugate, the hours of sunlight at Faraday and its conjugate. (Reprinted from Saxton, J.M., Smith, A.J., 1989. Quiet time plasmaspheric electric fields and plasmasphere–ionosphere coupling fluxes. *Planetary and Space Science*, Vol. 37, pp. 283–293, with permission from Elsevier Science.)

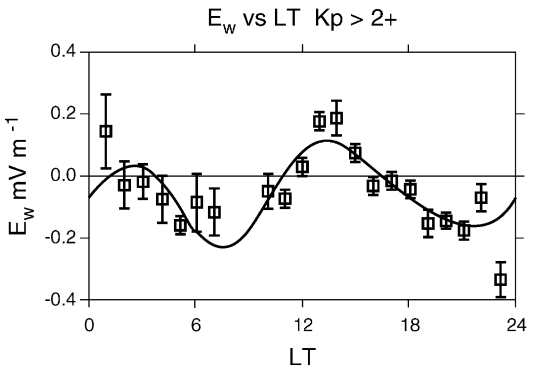

Fig. 15. Similar to Fig. 14 but for disturbed times $K_p > 2+$) during eight nights in June/July 1986. The difference between the mean of the third-order harmonic fit to the data and the theoretical zero mean can be accounted for by the small sample and the fact that we are biasing the observations to the upper range of K_p, not averaging over all levels of magnetic activity. (Reprinted from Saxton, J.M., Smith, A.J., 1991. Electric fields at $L = 2.5$ during geomagnetically disturbed conditions. *Planetary and Space Science*, Vol. 39, pp. 1305–1320, with permission from Elsevier Science.)

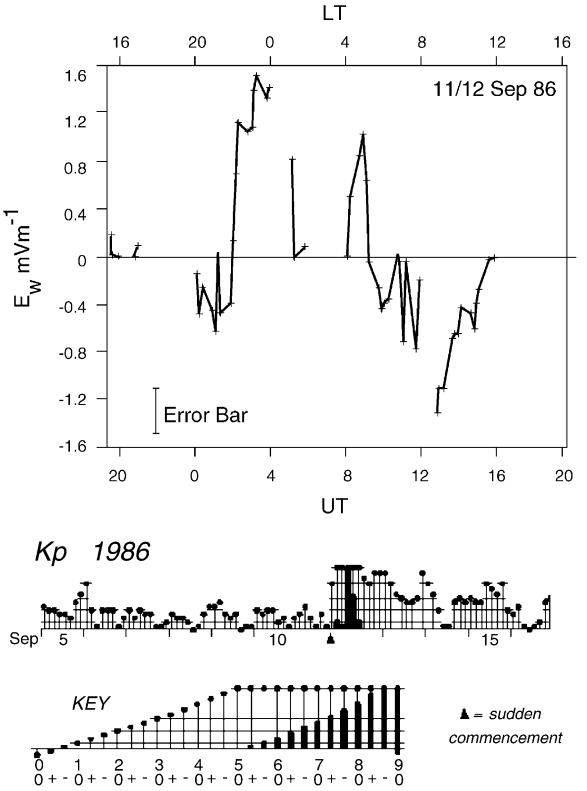

Fig. 16. Zonal plasmaspheric electric field results for 11–12 September 1986 at Faraday ($L \sim 2.5$). A large magnetic storm had its sudden commencement at about 22 UT, as indicated in the plot of the K_p index, which reached a maximum of 9 – during the storm (reproduced from Fig. 4 of Balmforth et al., 1994).

stable duct structures). Nevertheless, it could be determined that the available data were consistent with an exponential relaxation of the field back to near the quiet-time level (compared with relaxation modeled by a step function or a damped oscillatory function). The model runs showed how the O^+–H^+ transition height and coupling flux were affected during the storm, relative to the average quiet-time behavior. The data for the May event were less continuous but suggested a rather different behavior, with an eastward field (outward drift) predominating. The contrast between the two cases was probably due to the differing universal times of the storm commencements.

Higher time resolution (5 s) observations of whistler mode signals from NAA, observed at Faraday by Yearby and Clilverd (1996), were used to measure the Doppler shift variations for six whistler ducts in the field of view of the receiver. Assuming the shifts were due to transverse motion of the ducts, a 13 mHz spectral component was interpreted as the passage of a hydromagnetic wave across the ducts. The amplitude and phase of this wave at each duct were used to infer the magnitude (920 km s^{-1}) and direction (from the afternoon magnetopause) of this 75 s period fast mode wave.

2.2. *Observations at L∼4 of signals from the Siple, Antarctica experimental transmitter*

Paschal (1988) applied digital processing techniques to recordings in Canada of signals propagating in the

$L = 3$–5 range from the Siple experimental VLF transmitter in Antarctica ($L \sim 4.2$) (Helliwell, 1988). The received signals often displayed fast temporal growth and stimulated emissions at new frequencies (e.g. Paschal and Helliwell, 1984), at which times their complex and rapid changes in phase made impossible identification of the effects of path drifts and/or interchange fluxes. Furthermore, because radiated power was small, from a few watts to a kilowatt, there was no measurable ground wave in the conjugate region to use as a reference. Nevertheless, there were occasions when signals up to 30 dB above the background noise were received without evidence of nonlinear effects (Paschal, 1988), and it was shown that at such times, order-of-1-s time resolution of Doppler shifts could be obtained and that transient hydromagnetic wave activity along the transmitter signal path could be detected. In a case in which four 2-s pulses at 3030 Hz were transmitted at 10-s intervals, Paschal (1988) plotted the log amplitude of the signals within a 20 Hz bandwidth and the phase with respect to a synthesized oscillator running at exactly 3030 Hz. The phase plots showed a Doppler shift that varied from ~ -0.10 to -0.20 Hz. Paschal considered the effects of duct drift and plasma flux, and using an analysis similar in concept to those performed previously by Thomson (1976a) and Andrews (1980), concluded that the dominant effect involved was an outward duct drift, as could be expected for the postdawn ($\sim$0730 MLT) local time and magnetically quiet conditions prevailing. The key point here is the order-of-1-s time resolution achieved with the Doppler shift measurements.

In another case, Paschal et al. (1990) were able to correlate changes in phase delay of Siple signals with a transient hydromagnetic wave present on the field line of Siple signal propagation.

3. Concluding remarks

Whistler-mode signals from lightning have been used with success to track cross-L bulk motions in the plasmasphere beyond $L \sim 3$. They have provided substantial new information on the spatially and temporally structured manner in which convection electric fields penetrate the plasmasphere. An example is the unexplained reversal in the cross-L plasma flow direction from inward to outward in the immediate aftermath of a temporally isolated substorm. Whistlers have also been useful in identifying the plasmaspheric drifts associated with quiet-day electric fields of ionospheric dynamo origin, and in showing that the GSE E_y, or duskward, component of the convection electric field in the outer plasmasphere is substantially larger near dusk than it is near mid-night.

Whistler-mode signals from transmitters have proven to be a powerful means of tracking cross-L motions in the plasmasphere near $L = 2.5$ while separately identifying the effects on the signal-phase paths of interchange fluxes with the ionosphere. When used as inputs to numerical models of the coupled plasmasphere–ionosphere system, results of such measurements have provided new geophysical insights.

Whistlers and man-made signals both have much unrealized potential as sources of information on plasmasphere dynamics. In the case of whistlers, modern methods of digital signal processing, including pattern recognition, as well as direction finding, could lead to multipoint tracking of plasma motions in both the cross-L and azimuthal directions. Work with communication transmitter signals can provide critical correlative information during future satellite campaigns involving photon or radio imaging of the plasmasphere. An experimental VLF transmitter near $L = 4$ could be used to measure cross-L plasma drifts in the outer plasmasphere with $\sim$1-s time resolution and to detect hydromagnetic waves on the field lines of signal propagation.

References

Akasofu, S.I., 1964. The development of the auroral substorm. Planetary Space Science 12, 273.

Andrews, M.K., 1980. Night-time radial plasma drifts and coupling fluxes at $L = 2.3$ from whistler mode measurements. Planetary Space Science 28, 407–417.

Andrews, M.K., Knox, F.B., Thomson, N.R., 1978. Magnetospheric electric fields and protonospheric coupling fluxes inferred from simultaneous phase and group path measurements on whistler-mode signals. Planetary Space Science 26, 171–183.

Angerami, J.J., 1966. A whistler study of the distribution of thermal electrons in the magnetosphere. Ph.D. Dissertation, Radioscience Laboratory, Stanford University.

Axford, W.I., Hines, C.O., 1961. A unifying theory of high-latitude geophysical phenomena and geomagnetic storms. Canadian Journal of Physics 39, 1433.

Balmforth, H.F., Moffett, R.J., Smith, A.J., Bailey, G.J., 1994b. The effect of disturbed-time electric fields on the inner plasmasphere. Annals of Geophysics 12, 296–303.

Balmforth, H.F., Clilverd, M.A., Smith, A.J., 1994a. A case study of storm commencement and recovery plasmaspheric electric fields near $L = 2.5$ at equinox. Annals of Geophysics 12, 625–635.

Block, L.P., Carpenter, D.L., 1974. Derivation of magnetospheric electric fields from whistler data in a dynamic geomagnetic field. Journal of Geophysical Research 79, 2783–2789.

Carpenter, D.L., 1966. Whistler studies of the plasmapause in the magnetosphere: 1. Temporal variations in the position of the knee and some evidence on plasma motions near the knee. Journal of Geophysical Research 71, 693–709.

Carpenter, D.L., 1968. Ducted whistler-mode propagation in the magnetosphere; a half-gyrofrequency upper intensity cutoff and some associated wave growth phenomena. Journal of Geophysical Research 73, 2919–2928.

Carpenter, D.L., 1970. Whistler evidence of the dynamic behavior of the duskside bulge in the plasmasphere. Journal of Geophysical Research 75, 3837–3847.

Carpenter, D.L., 1978. New whistler evidence of a dynamo origin of electric fields in the quiet magnetosphere. Journal of Geophysical Research 83, 1558–1564.

Carpenter, D.L., 1981. A study of the outer limits of ducted whistler propagation in the magnetosphere. Journal of Geophysical Research 86, 839–845.

Carpenter, D.L., Akasofu, S.I., 1972. Two substorm studies of relations between westward electric fields in the outer plasmasphere, auroral activity, and geomagnetic perturbations. Journal of Geophysical Research 77, 6854–6863.

Carpenter, D.L., Bao, Z.T., 1983. Occurrence properties of ducted whistler-mode signals from the new VLF transmitter at Siple Station, Antarctica. Journal of Geophysical Research 88, 7051.

Carpenter, D.L., Miller, T.R., 1976. Ducted magnetospheric propagation of signals from the Siple, Antarctica, VLF transmitter. Journal of Geophysical Research 81, 2692.

Carpenter, D.L., Park, C.G., Miller, T.R., 1979. A model of substorm electric fields in the plasmasphere based on whistler data. Journal of Geophysical Research 84, 6559–6563.

Carpenter, D.L., Seely, N.T., 1976. Cross-L plasma drifts in the outer plasmasphere: quiet time patterns and some substorm effects. Journal of Geophysical Research 81, 2728–2736.

Carpenter, D.L., Stone, K., 1967. Direct detection by a whistler method of the magnetospheric electric field associated with a polar substorm. Planetary Space Science 15, 395–397.

Carpenter, D.L., Stone, K., Siren, J.C., Crystal, T.L., 1972. Magnetospheric electric fields deduced from drifting whistler paths. Journal of Geophysical Research 77, 2819–2834.

Gonzales, C.A., Kelley, M.C., Carpenter, D.L., Miller, T.M., Wand, R.H., 1980. Simultaneous measurements of ionospheric and magnetospheric electric fields in the outer plasmasphere. Geophysical Research Letters 7, 517–520.

Hayakawa, M., Ohta, K., Shimakura, S., 1992. Direction finding techniques for magnetospheric VLF waves; recent achievements. Trends in Geophysical Research 1, 157–164.

Helliwell, R.A., 1963. Coupling between the ionosphere and the earth-ionosphere waveguide at very low frequencies. In Proceedings of the International Conference on the Ionosphere, London, July 1962. Bartholomew Press, Dorking, England.

Helliwell, R.A., 1965. Whistlers and Related Ionospheric Phenomena. Stanford University Press, Stanford, CA.

Helliwell, R.A., 1974. Controlled VLF wave injection experiments in the magnetosphere. Space Science Reviews 15, 781–802.

Helliwell, R.A., 1988. VLF wave stimulation experiments in the magnetosphere from Siple Station, Antarctica. Reviews of Geophysics 26, 551.

Helliwell, R.A., Carpenter, D.L., 1961. Whistlers-West IGY synoptic program. Final Report, Radioscience Laboratory, Stanford University.

Helliwell, R.A., Gehrels, E., 1958. Observations of magneto-ionic duct propagation using man-made signals of very low frequency. Proceedings of IRE 46 (10), 1760–1762.

Kasaba, Y., Matsumoto, H., Hashimoto, K., Anderson, R.R., Bougeret, J.-L., Kaiser, M.L., Wu, X.Y., Nagano, I., 1988. Remote sensing of the plasmapause during substorms: geotail observation of nonthermal continuum enhancement. Journal of Geophysical Research 103, 20,389–20,405.

Kelley, M., 1989. The Earth's Ionosphere. Academic, San Diego, CA.

Kimura, I., 1968. Triggering of VLF magnetospheric noise by a low power ($\sim$100 watts) transmitter. Journal of Geophysical Research 73, 445.

Kivelson, M.G., 1976. Magnetospheric electric fields and their variations with geomagnetic activity. Reviews of Geophysics and Space Physics 14, 189–197.

Leavitt, M.K., Carpenter, D.L., Seely, N.T., Padden, R.R., Doolittle, J.H., 1978. Initial results from a tracking receiver direction finder for whistler mode signals. Journal of Geophysical Research 83, 1601.

Machida, S., Tsuruda, K., 1984. Intensity and polarization characteristics of whistlers deduced from multi-station observations. Journal of Geophysical Research 89, 1675–1682.

Maynard, N.C., Aggson, T.L., Heppner, J.P., 1983. The plasmaspheric electric field as measured by ISEE 1. Journal of Geophysical Research 88, 3981.

McNeill, F.A., 1967. Frequency shifts on whistler mode signals from a stabilised VLF transmitter. Radio Science 2, 589–594.

McNeill, F.A., Andrews, M.K., 1975. Quiet-time characteristics of middle-latitude whistler-mode signals during an 8-yr period. Journal of Atmospheric and Terrestrial Physics 37, 531–543.

Mozer, F.S., 1970. Electric field mapping from the ionosphere to the equatorial plane. Planetary Space Science 18, 259.

Park, C.G., 1972. Methods of determining electron concentrations in the magnetosphere from nose whistlers. Technical Report No. 3454-1, Radioscience Laboratory, Stanford University.

Paschal, E.W., 1988. Phase measurements of very low frequency signals from the magnetosphere. Ph.D. Thesis, Stanford University.

Paschal, E.W., Helliwell, R.A., 1984. Phase measurements of whistler mode signals from the Siple VLF transmitter. Journal of Geophysical Research 89, 1667–1674.

Paschal, E.W., Lanzerotti, L.J., Maclennan, C.G., 1990. Correlation of whistler mode phase delay with transient hydromagnetic waves. Journal of Geophysical Research 95, 15,059–15,071.

Rostoker, G., Hron, M., 1975. The eastward electrojet in the dawn sector. Planetary Space Science 23, 1377–1389.

Saxton, J.M., Smith, A.J., 1989. Quiet time plasmaspheric electric fields and plasmasphere-ionosphere coupling fluxes at $L = 2.5$. Planetary Space Science 37, 283–293.

Saxton, J.M., Smith, A.J., 1991. Electric fields at $L = 2.5$ during magnetically disturbed conditions. Planetary Space Science 39, 1305–1320.

Shklyar, D.R., Nunn, D., Smith, A.J., Sazhin, S.S., 1992. An investigation into the nonlinear frequency shift in magnetospherically propagated VLF pulses. Journal of Geophysical Research 97, 19,389–19,402.

Smith, A.J., Yearby, K.H., Bullough, K., Saxton, J.M., Strangeways, H.J., Thomson, N.R., 1987. Whistler mode signals from VLF transmitters observed at Faraday, Antarctica. Memoirs of the National Institute of Polar Research Special Issue 48, 183–195.

Smith, R.L., 1961a. Propagation characteristics of whistlers trapped in field-aligned columns of enhanced ionization. Journal of Geophysical Research 66, 3699.

Smith, R.L., 1961b. Properties of the outer ionosphere deduced from nose whistlers. Journal of Geophysical Research 66, 3709.

Thomson, N.R., 1976a. Causes of the frequency shift of whistler-mode signals. Planetary Space Science 24, 447–454.

Thomson, N.R., 1976b. Electric fields from whistler-mode Doppler shifts. Planetary Space Science 24, 455–458.

Thomson, N.R., 1981. Whistler mode signals: spectrographic group delays. Journal of Geophysical Research 86, 4795–4802.

Vasyliunas, V.M., 1968. A crude estimate of the relations between the solar wind speed and the magnetospheric electric field. Journal of Geophysical Research 73, 2529.

Wygant, J., Rowland, D., Singer, H.J., Temerin, M., Mozer, F., Hudson, M.K., 1998. Experimental evidence on the role of the large spatial scale electric field in creating the ring current. Journal of Geophysical Research 103, 29,527–29,544.

Yearby, K.H., Clilverd, M.A., 1996. Doppler shift pulsations on whistler mode signals from a VLF transmitter. Journal of Atmospheric and Terrestrial Physics 58, 1489–1496.